COMPUTED TOMOGRAPHIC IMAGING OF PEDIATRIC ORBITS

Kanokporn ORANRATANACHAI, Noppaklao MANOWATANA, Malai MUTTARAK, Pannee VISRUTARATNA, Wantana PRAPAKORN

ABSTRACT

From January 1995 to December 1996, computed tomographic imaging of the orbits was performed on 48 pediatric patients at the Department of Radiology, Faculty of Medicine, Chiang Mai University. Pathological and/or clinical proofs of diagnoses were successfully obtained from only 35 of these patients, in whom ocular (n=21) and orbital (n=14) diseases were found. These ocular diseases included retinoblastoma (n=14) and non-tumoral retinal detachment (n=3); the remainder were persistent hypertrophic primary vitreous, congenital glaucoma, intraocular foreign body, and posttraumatic lens aspiration. The orbital diseases included acute myeloblastic leukemia (n=3), preseptal cellulitis (n=3), neurofibroma (n=2); the remainder were neuroblastoma, primitive neuroectodermal tumor, rhabdomyosarcoma, capillary hemangioma, orbital cellulitis, and optic neuritis. The computed tomographic findings of these patients are reviewed and discussed.

INTRODUCTION

Imaging is particularly important and useful in the very young child when clinical evaluation of visual functions is difficult and may not be precise. Computed tomography (CT) represents an important form of imaging for the evaluation of the pediatric eye and orbit, since orbital fat provides excellent natural contrast for the demonstration of soft tissue structures.[1] In addition, bony details and calcification are also well demonstrated by CT.[2] The axial and coronal sectional imagings provided by CT are well suited for the depiction of the complex anatomic relationships of orbital structures.

MATERIALS AND METHODS

From January 1995 to December 1996, CT of the orbits were performed on 48 pediatric patients in the Department of Radiology, Chiang Mai University Hospital. Thirty-five patients who had had pathological and/or clinical diagnoses of orbital abnormalities were retrospectively studied. In all cases, the plain CT scans were performed on a GE Sytec 3000i scanner with the X-ray beam at 0 or -10 degree from the orbitomeatal line with 5 mm slice thickness. Postcontrast axial scans were obtained in 32 cases. The 5 mm thick coronal scans were performed after enhanced axial scans in 15 cases.

The cases were divided into two groups, those with ocular and those with orbital diseases, according to the location of the lesions on CT scans. Ocular disease was defined as lesions which originated within the eye globe, orbital disease as lesions arising in the extraocular orbital compartment.

Department of Radiology, Faculty of Medicine, Chiang Mai University, Chiang Mai 50200 Thailand

RESULTS

There were 17 boys and 18 girls, ranging from 2 months to 14 years of age. The CT scans demonstrated ocular diseases in 21 and orbital diseases in 14 (Table 1).

The ocular diseases (Table 2) included retinoblastoma (n=14) and non-tumoral retinal detachment (RD) (n=3); the remainder were persistent hypertrophic primary vitreous (PHPV), congenital glaucoma, intraocular foreign body (FB) and posttraumatic lens aspiration.

The orbital diseases included 8 orbital tumors (Table 3); the remainder (Table 4) were preseptal cellulitis (n=3), orbital cellulitis, optic neuritis, and capillary hemangioma.

TABLE 1: Location of disease in CT scan

DISEAES	No. of patients
I. OCULAR DISEASES	21
A. Congenital malformation:	
Congenital glaucoma	1
PHPV	1
B. Vitreoretinal disorder:	
Retinal detachment	3
C. Tumor:	
Retinoblastoma	14
D. Trauma:	
Intraocular foreign body	1
Posttraumatic lens aspiration	1
II.. ORBITAL DISEASE	14
A. Infection:	
Preseptal cellulitis	3
Orbital cellulitis	1
B. Inflammation:	
Optic neuritis	1
C. Vascular lesion:	
Capillary hemangioma	1
D. Tumor:	
Acute myeloblastic leukemia	3
Neurofibroma	2
Neuroblastoma	1
Primative neuroectodermal tumor	1
Rhabdomyosarcoma	1

TABLE 2: Clinical and CT findings of ocular diseases

patient & age	sex	presenting symptoms	site	globe: S,N,L	No. of masses	margin	calci-fication	enhance-ment	extraocular extension	diagnosis
1. 1 y	F	leukokoria	RE	N	single	good	+	+	none	retinoblastoma
2. 3 y	F	leukokoria	RE	N	single	good	+	+	none	retinoblastoma
3. 2 m	F	leukokoria	RE	N	single	good	+	+	none	retinoblastoma
4. 2 m	M	leukokoria	BE	N,L	multiple	good	+	+	none	retinoblastoma
5. 2 y	F	leukokoria	LE	N	single	good	+	+	none	retinoblastoma
6. 14 m	F	leukokoria	BE	L,L	multiple	good	+	+	none	retinoblastoma
7. 2 y	F	leukokoria	LE	N	single	good	+	+	none	retinoblastoma
8. 9 y	F	blindness	LE	N	multiple	poor	+	+	optic nerve	retinoblastoma
9. 8 y	F	proptosis	RE	L	single	poor	+	+	optic nerve & soft tissue	retinoblastoma
10. 1 y	M	leukokoria	LE	L	single	good	+	+	optic nerve	retinoblastoma
11. 2 y	M	leukokoria	RE	S	single	poor	+	+	leptomeningeal invasion	retinoblastoma
12. 3 m	F	leukokoria	RE	N	singlr	good	+	+	none	retinoblastoma
13. 1 y	F	leukokoria	LE	N	multiple	good	+	+	lacrimal gland	retinoblastoma
14. 1 y	F	leukokoria	BE	N	multiple	good	+	+	none	recurrent retinoblastoma
15. 7 y	F	leukokoria	LE	S	single	-	-	+	none	PHPV
16. 4 y	F	leukokoria	RE	N	no mass	-	-	-	-	RD
17. 8 y	M	leukokoria	RE	N	no mass	-	-	-	-	RD
18. 5 y	M	leukokoria	RE	N	no mass	-	-	-	-	RD
19. 4 m	M	cataract	LE	L	no mass	-	-	-	-	congenital glaucoma
20. 14 y	M	trauma	LE	N	FB	good	metal	-	none	intraocular FB
21. 2 y	M	trauma	LE	N	no mass	-	-	-	-	posttraumatic lens aspiration

RE = right eye, LE =left eye, BE = both eye

S = small, N = normal, L = large

TABLE 3: CT findings of orbital tumors

	No. of Patients	Proptosis	Bone Change	Location	Well-defined Margin	Infiltration		Attenuation			Enhancement	
						Muscle	Nerve	Hyper-dense	Iso-dense	Hypo-dense	Homo-geneous	Hetero-geneous
Acute myeloblastic leukemia	3	3	2	Extraconal 1 Extra-and intra-conal 1 Lacrimal gland 1	2	1	1	3	0	0	3	0
Neurofibroma	2	1	0	Extraconal 1 Extra-and intra-conal 1	1	0	0	1	1	0	0	2
Neurofibroma	1	1	1	Extraconal 1	1	0	0	1	0	0	1	0
Primitive neuroectodermal tumor	1	1	0	Extra-and intra-conal 1	1	1	1	1	0	0	1	0
Rhabdomyosarcoma	1	1	0	Extra- and intra-conal 1	1	1	0	1	0	0	1	0

TABLE 4: CT findings of non-tumoral orbital lesions.

DISEASES	No. of patients	CT findings
Preseptal cellulitis	3	Swelling and enhancement of preseptal soft tissue,
Orbital cellulitis	1	Proptosis and swelling of left periorbital soft tissue. superomedial extraconal mass and enlarged left medial rectus and superior rectus muscles, opacified left maxillary and ethmoid sinuses.
Optic neuritis	1	Uniformly enlarged, enhanced left optic nerve.
Capillary hemangioma	1	Hyperdense enhanced extraconal lesion.

DISCUSSION

The spectrum of ocular and orbital pathology in the pediatric age group is quite different from that seen in adults.[1,3]

Retinoblastoma is the most common primary intraocular malignant tumor of childhood.[2,4-7] There were 14 cases of this tumor with pathologically proven retinoblastoma, which is the most common ocular disease (14/21 = 66%). This was the only ocular tumor in this study. These affected 10 girls and 4 boys, ranging from 2 months to 9 years of age. Most of the patients (12) were younger than 4 years of age. The most frequent presenting symptom was leukokoria (n=12). Three cases had bilateral retinoblastoma (Fig.1). In all cases, the CT findings showed iso- to hyperdense intraocular enhanced mass(es) with calcification. Almost all of the tumors were well defined. Multifocal lesions were seen in 5 patients, including three with bilateral retinoblastoma. The affected globes were either normal in size (n=10) or enlarged (n=5). Only one small globe appeared in our study. Recurrent retinoblastoma in a postenucleated eye was seen in one case of bilateral retinoblastoma. Of the cases with extraocular invasion (n=5), three had extension of the tumor along the optic nerve (Fig.2) and retrobulbar soft tissue, one had leptomeningeal involvement, and the remainder had lacrimal gland involvement. Clinically it is frequently difficult to differentiate retinoblastoma from benign diseases causing leukokoria such as PHPV, Coat's disease and toxocara endophthalmitis.[3,6-8] CT is essential for the radiologic diagnosis of retinoblastoma, primarily because it is most sensitive to calcification, an important feature distinguishing retinoblastoma from other entities.[7] The presence of intraocular calcification in children under 3 years of age is highly suggestive of retinoblastoma.[5-7] Retinoblastoma is seen on CT as an intraocular mass lesion which is calcified in about 95% of cases and located posterior to the lens. There is usually mild or moderate enhancement of the tumor which helps to separate the tumor from accompanying subretinal effusion. Bilateral retinoblastoma occasionally may be associated with a pineal neuroectodermal tumor, a so-called trilateral retinoblastoma.[3,7] Three of our patients had bilateral retinoblastoma without evidence of pineal tumor. CT readily reveals the size of the intraocular lesion and the important role of CT is the delineation of the retro-orbital extent of the tumor and determining if the optic nerve is involved or if there is intracranial extension[4]. This information is of prognostic value, as patients with tumors that have spread beyond the confines of the globe have a life expectancy of only a few months.[4] The most common route of extraocular extension is along the optic nerve; there can be extension into the subarachnoid space.

PHPV is the second most common cause of leukokoria, but we had only one case (Fig.3). Theoretically, PHPV results from failure of a portion of the embryonic intraocular vascular system to involute. CT findings of PHPV are microphthalmia, diffuse high attenuation appearance of the vitreous with intense enhancement of a thin, triangular or S-shape band in the vitreous. The enhanced band consists of remnants of the hyaloid vascular system. Other reported findings have been a small optic nerve and vitreous fluid-fluid levels of differing attenuation resulting from the recurrent hemorrhage in the subhyaloid or subretinal space.[8] PHPV can be differentiated from retinoblastoma by the presence of microphthalmia and absence of calcification within the globe.[1,7,8]

CT is important in the diagnosis of intraocular foreign bodies.[1,2] A metallic foreign body as small as 5 mm in diameter was detected in one of our cases by CT with a slice thickness of 5 mm. By this means, it is also possible to accurately determine the location of a radiopaque foreign body in relation to the globe.

Abnormalities that occur in the infected orbit were classified according to the involved structures and compartments, i.e. the preseptal soft tissues, and the intraconal, extraconal and subperiosteal compartments.[2] In our study, preseptal cellulitis was the most common manifestation of an orbital infection (Fig.4). Anatomically, the orbital septum serves as a barrier to the extension of disease into the orbital proper. Therefore, an important function of CT in this condition is to detect extension of disease into the orbit proper and to evaluate the paranasal sinuses.[1] Orbital cellulitis usually involves both the preseptal tissues as well as extraconal compartment of orbital structures, as seen in one of our cases (Fig.5). Acute inflammation of the orbit is frequently secondary to extension from the ethmoid sinusitis. Both inflammatory edema and cellulitis were demonstrated with CT as increased attenuation of orbital fat and enlargement of the extraocular muscles.[1,9] A medial extraconal soft-tissue mass that caused proptosis and lateral displacement of the globe and optic nerve was easily recognized on CT.

There were 8 pathologically proven orbital tumors in our studies (Table 3). Almost all of these patients had proptosis. The most of the tumors had extraconal hyperdense mass with homogeneous enhancement and well-defined margin. Bone destruction was seen in two cases of acute myeloblastic leukemia (Fig.6) and in one case of neuroblastoma (Fig.7), all of which were aggressive secondary tumors of the orbit. Acute myeloblastic leukemia was the most common orbital tumor in our study. However, rhabdomyosarcoma of the orbit, which is the most common orbital malignancy in children, was found in only one of our cases (Fig.8). There were only 5 different histological types of tumors in our study with the number of cases ranging from 1 to 3; therefore these data cannot be considered representative of the complete CT spectrum. Although CT scans do not permit the specific feature or accurately diagnose orbital tumors, CT scans do detect them and show extension, particularly in the retrobulbar space, in patients with proptosis.[10,11] The tumor masses can be located and identified according to their relation to the muscular cone. Bone destruction is often present with aggressive lesions.

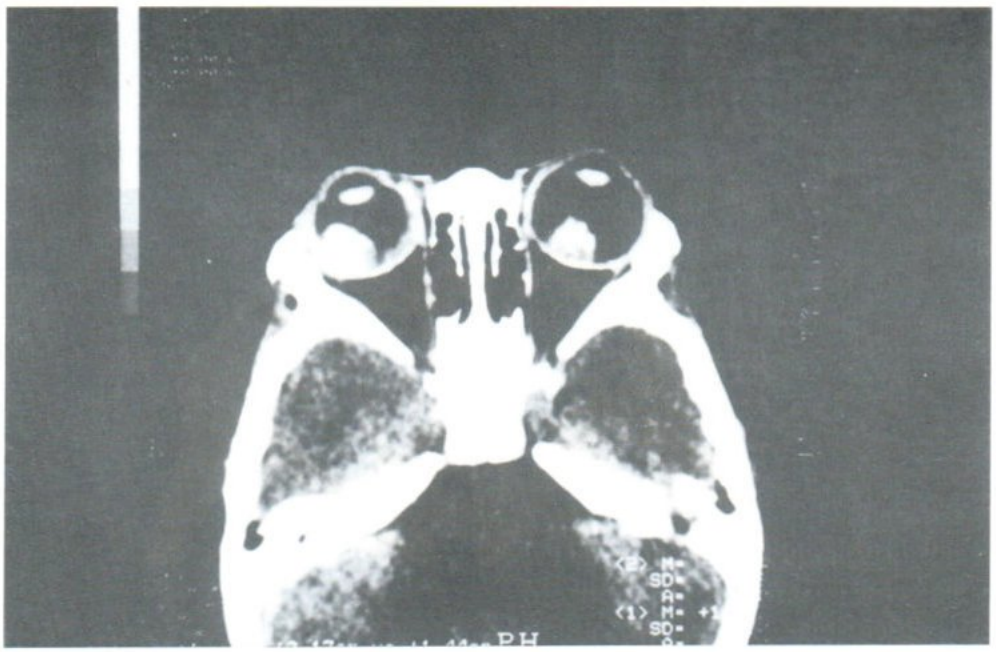

Fig.1 Bilateral Retinoblastoma: CT scan demonstrates bilateral intraocular masses. A portion of both masses is densely calcified.

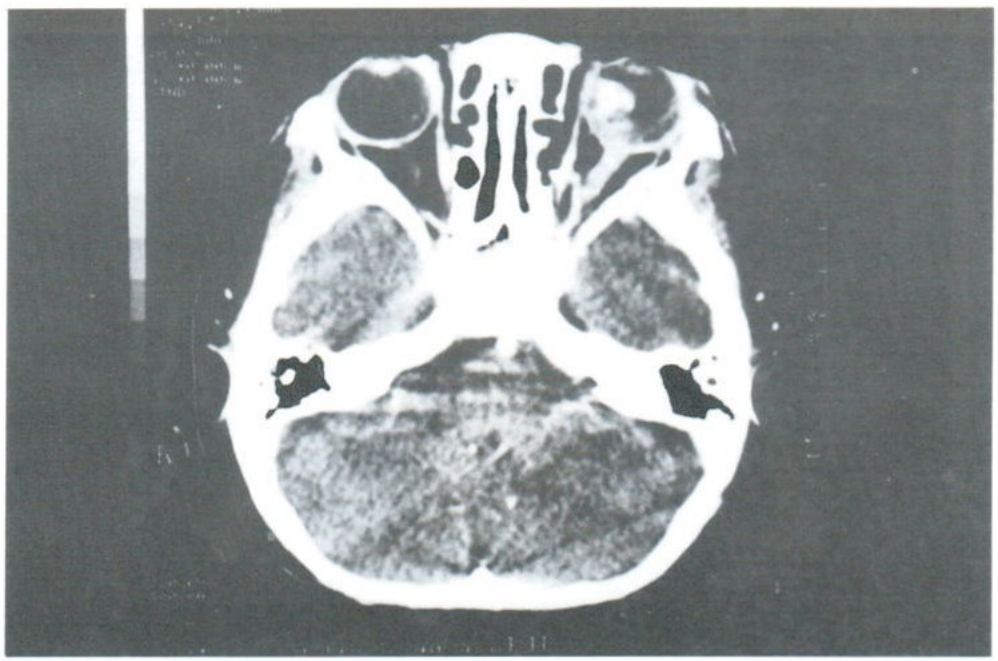

Fig.2 Retinoblastoma of left eye involves optic nerve.

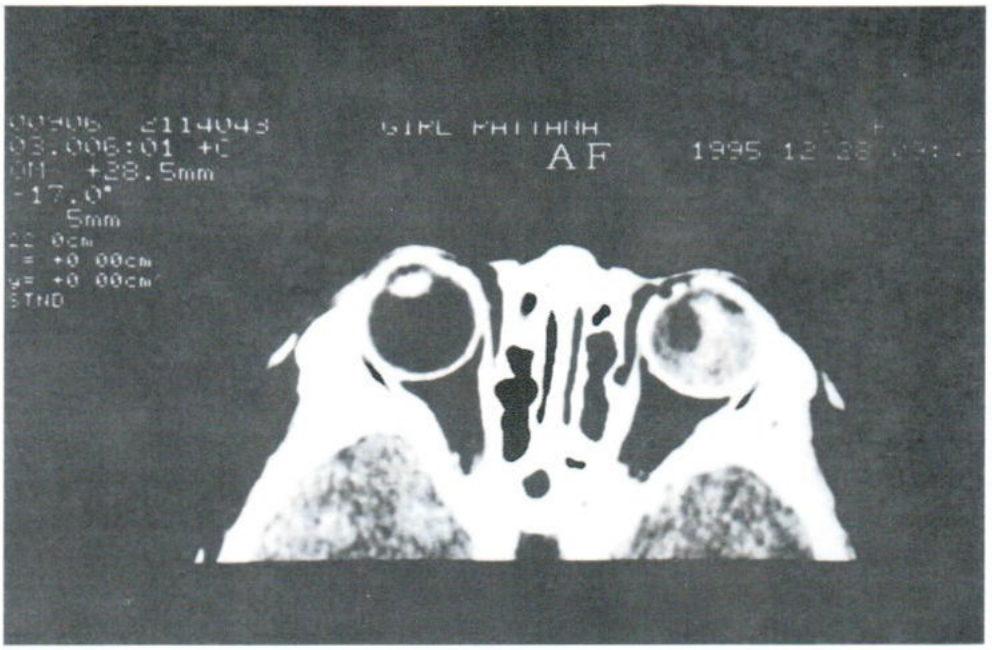

Fig.3 PHPV: There is enhanced retrolental S-shaped mass that represents the hyperplastic primary vitreous of left eye. The accompanying retinal detachment is seen as nonenhanced hyperattenuating area.

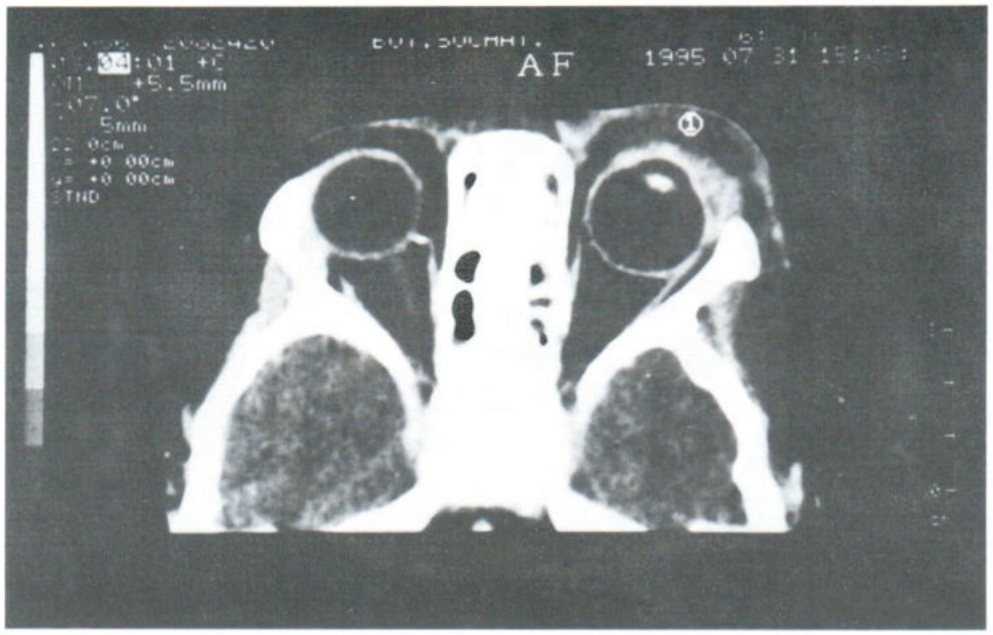

Fig.4 Preseptal Cellulitis: Axial CT scan shows diffuse soft tissue swelling involving the lid and conjunctiva anterior to the orbital septum.

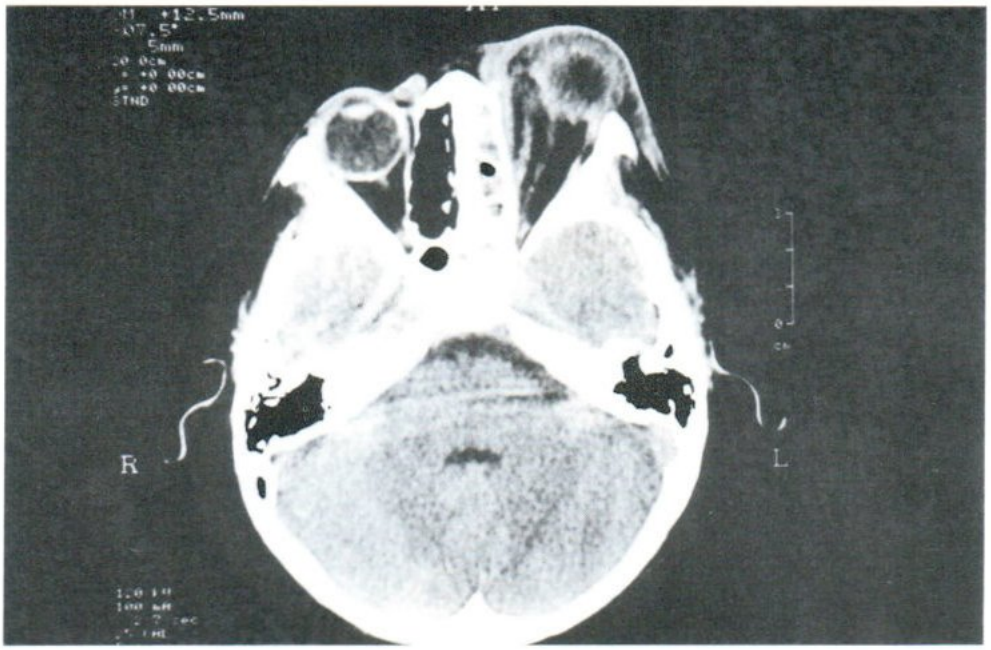

Fig.5 Orbital Cellulitis: Axial CT scan shows inflammatory edema of periorbital soft tissue and medial extraconal compartment of left orbit secondary to ethmoid sinusitis.

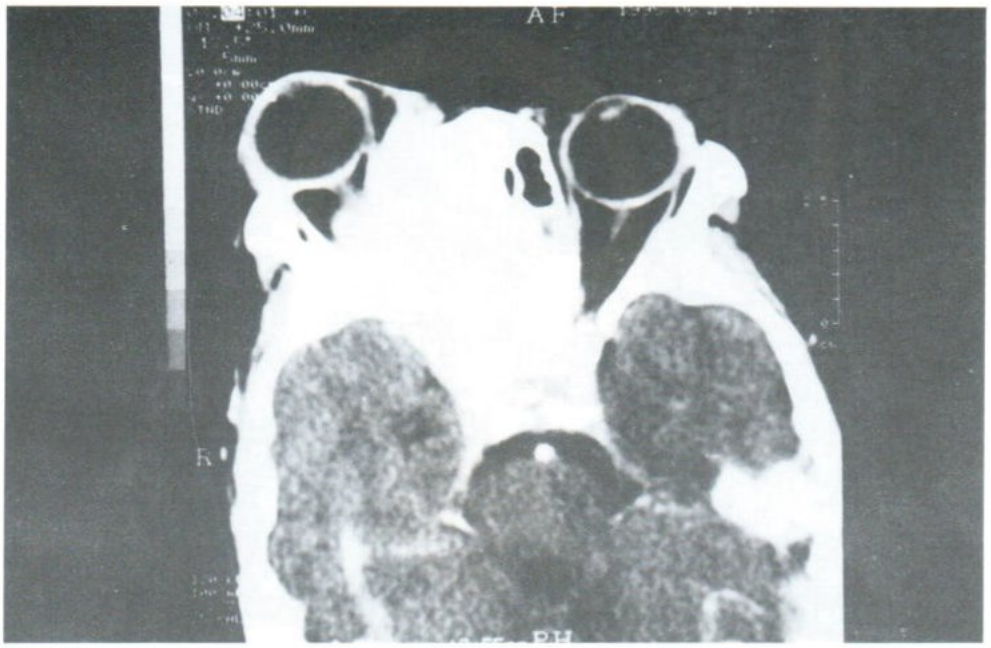

Fig.6 Acute Myeloblastic Leukemia: CT scan of 8-year-old girl shows large, enhanced, infiltrative mass involving paranasal sinuses with bone destruction and extension into both extra- and intraconal spaces of right orbit.

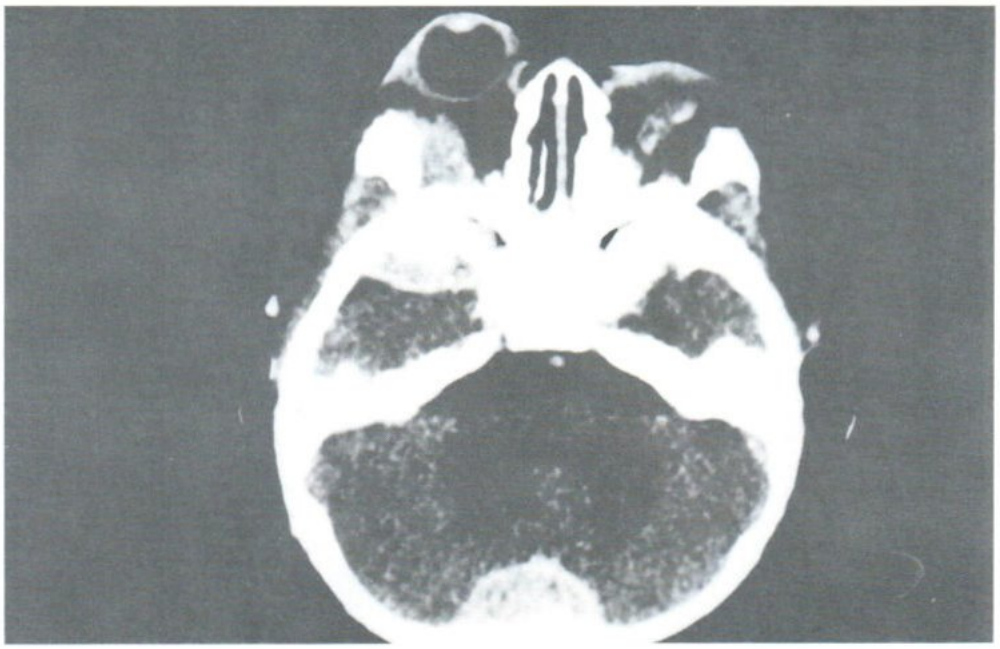

Fig.7 Neuroblastoma: CT scan of 3-year-old boy shows bone involvement from metastatic neuroblastoma with extraconal extension.

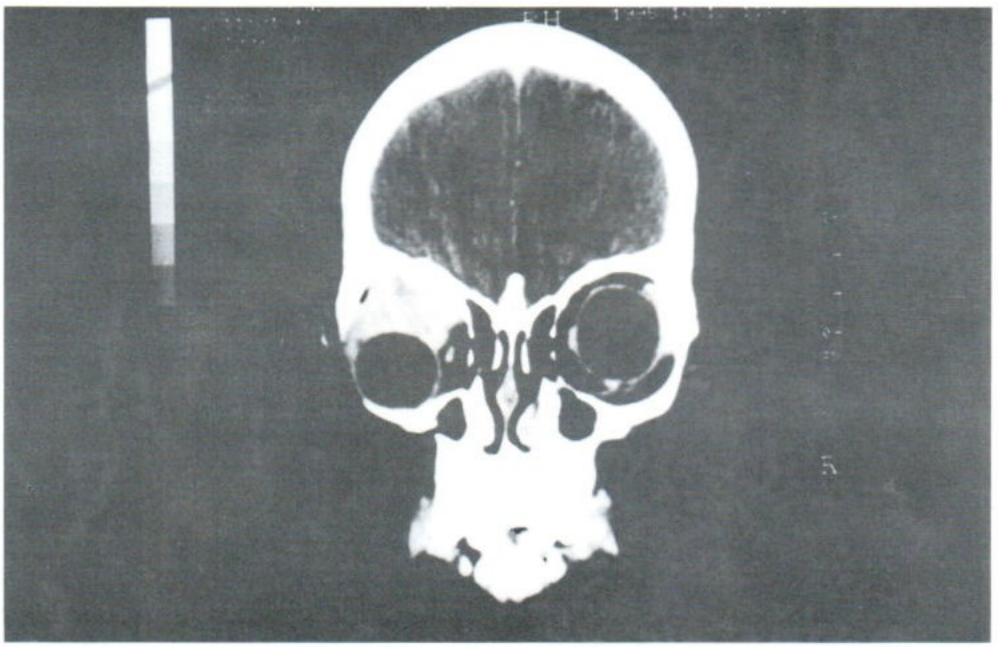

Fig.8 Rhabdomyosarcoma: Coronal CT scan shows homogeneous enhanced left orbital mass.

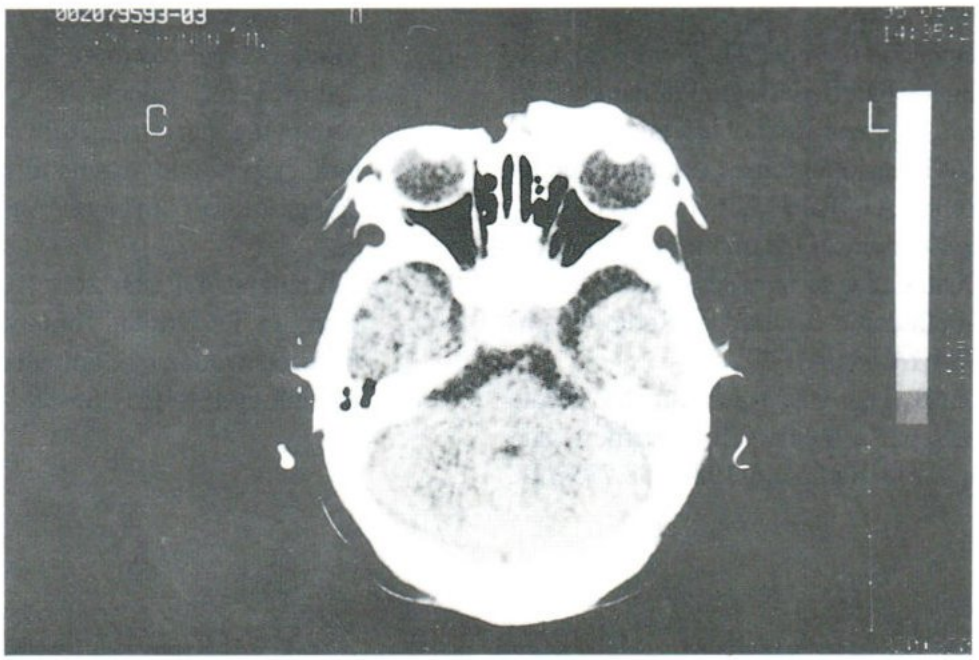

Fig.9 Capillary Hemangioma: CT scan of 2-month-old boy shows lobulated, markedly enhanced extraconal mass.

CONCLUSION

We reviewed the CT of pediatric orbits in 35 patients; 21 had ocular diseases and 14 had orbital diseases. Retinoblastoma was the most common ocular disease and the only ocular tumor in our study. In the orbital group, orbital tumor was found to be the most common lesion.

We found that CT is the optimal imaging for demonstration and delineation of lesions in pediatric orbits. Bony detail and calcification show up very well on CT. Particularly in retinoblastoma CT is considered to be the imaging of choice in children under 3-4 years of age who have leukokoria.

REFERENCES

1. Wells RG, Sty JR, Gonnering RS: Imaging of the pediatric eye and orbit. RadioGraphics 1989;9:1023-1043.
2. Bilaniuk LT, Atlas SW, Zimmerman RA: The orbit. In: Lee SW, Rao K C.V.G., Zimmerman RA, eds. Cranial MRI and CT, 3rd ed.,1992;119-191.
3. Hopper KD, Sherman JL, Boal DK, Eggli KD: CT and MR imaging of pediatric orbit. RadioGraphics 1992;12:485-503.
4. Danziger A, Price HI: CT Findings in Retinoblastoma. AJR 1979;133:783-785.
5. Mafee MF, Schatz CJ: The orbit. In: Som PM, Bergeron RT, eds. Head and Neck Im aging, 2nd ed. St. Louis, Mosby, 1991;693-827.
6. Mafee MF, Goldberg MF, Greenwald MJ, et al: Retinoblastoma and simulating lesions: Role of CT and MR imaging. Radiol Clin North Am 1987; 25:667-682.

7. Provenzale JM, Weber AL, Klintworth GK, McLendon RE: Radiologic-Pathologic Correlation: Bilateral Retinoblastoma with Coexistent Pinealoblastoma (Trilateral Retinoblastoma). AJNR 1995;16:157-165.
8. Smirniotopoulos JG, Bargallo N, Mafee MF: Differential diagnosis of leukokoria: Radiologic-Pathologic correlation. Radio-Graphics 1994;14:1059-1079.
9. Towbin R, Han BK, Kaufman RA, Burke M: Postseptal cellulitis: CT in diagnosis and management. Radiology 1986;158:735-737.
10. Mafee MF, Putterman A, Valvassori GF, Campos M, Capek V: Orbital space-occupying lesions: Role of computed tomography and magnetic resonance imaging. Radiol Clin North Am 1987;25:529-559.
11. Lallemand DP, Brasch RC, Char DH, Norman D: Orbital Tumors in Children: Characterization by Computed Tomography. Radiology 1984;151:85-88.